The FEBS Journal

Low doses of paclitaxel enhance liver metastasis of breast cancer cells in the mouse model

Qi Li[1], Zhuang Ma[2], Yinhua Liu[3], Xiaoxi Kan[1], Changjun Wang[2], Bingnan Su[2], Yuchen Li[2], Yingmei Zhang[2], Pingzhang Wang[2], Yang Luo[2], Daxiang Na[2], Lanlan Wang[2], Guoying Zhang[2], Xiaoxin Zhu[1] and Lu Wang[2]

1 Institute of Chinese Materia Medica, China Academy of Chinese Medical Sciences, Beijing, China
2 Department of Immunology, Center for Human Disease Genomics, School of Basic Medical Science, Peking University Health Science Centre, Beijing, China
3 Surgery Department, Peking University First Hospital, Beijing, China

Keywords
breast cancer metastasis; cancer related inflammation; epithelial–mesenchymal transition; estrogen metabolism; paclitaxel

Correspondence
L. Wang, 38 Xueyuan Road, Haidian District, 100191 Beijing, China
Fax: 86 (10) 64013396
Tel: 86 (10) 82801417
E-mail: wanglu@bjmu.edu.cn
and
X. Zhu, 16 DongZhiMen South Street, Dongcheng District, 100700 Beijing, China
Fax: 86 (10) 64013396
Tel: 86 (10) 64056154
E-mail: zhuxiaoxin@icmm.ac.cn

(Received 22 January 2016, revised 13 May 2016, accepted 30 May 2016)

doi:10.1111/febs.13767

Paclitaxel is the most commonly used chemotherapeutic agent in breast cancer treatment. In addition to its well-known cytotoxic effects, recent studies have shown that paclitaxel has tumor-supportive activities. Importantly, paclitaxel levels are not maintained at the effective concentration through one treatment cycle; rather, the concentration decreases during the cycle as a result of drug metabolism. Therefore, a comprehensive understanding of paclitaxel's effects requires insight into the dose-specific activities of paclitaxel and their influence on cancer cells and the host microenvironment. Here we report that a low dose of paclitaxel enhances metastasis of breast cancer cells to the liver in mouse models. We used microarray analysis to investigate gene expression patterns in invasive breast cancer cells treated with low or clinically relevant high doses of paclitaxel. We also investigated the effects of low doses of paclitaxel on cell migration, invasion and metastasis *in vitro* and *in vivo*. The results showed that low doses of paclitaxel promoted inflammation and initiated the epithelial–mesenchymal transition, which enhanced tumor cell migration and invasion *in vitro*. These effects could be reversed by inhibiting NF-κB. Furthermore, low doses of paclitaxel promoted liver metastasis in mouse xenografts, which correlated with changes in estrogen metabolism in the host liver. Collectively, these findings reveal the paradoxical and dose-dependent effects of paclitaxel on breast cancer cell activity, and suggest that increased consideration be given to potential adverse effects associated with low concentrations of paclitaxel during treatment.

Database
Gene expression microarray data are available in the GEO database under accession number GSE82048.

Introduction

With one million new cases worldwide each year, breast cancer is the most common malignancy and ranks second in cancer mortality for women [1]. Strikingly, the main cause of death for breast cancer is not

Abbreviations
4-OHE2, 4-hydroxyestradiol; CCL20, chemokine (C-C motif) ligand 20; COMT, catechol-O-methyltransferase; CXCL1, chemokine (C-X-C motif) ligand 1; CYP, cytochrome P450; EMT, epithelial-mesenchymal transition; ICAM1, intercellular adhesion molecule 1; IKK, IκB kinase; IL, interleukin; NF-κB, nuclear factor-κB; PTX, paclitaxel; TNF, tumor necrosis factor; VCAM1, vascular cell adhesion molecule 1.

the primary tumor, but its metastasis [2,3]. Based on the century-old 'soil and seeds' theory, the interaction between metastatic cells and the microenvironment in host organs is critical for the formation of lethal metastases with organ specificity [4–8]. Clinically, breast cancer is preferable to dissemination to lungs, liver, brain and bones [9]. Among these four organs, liver is the third most susceptible site, and breast cancer with liver metastasis is statistically proven to be the predictive factor for drug resistance and poor prognosis [10–12].

Until now, despite the intense debate regarding its efficacy and safety, chemotherapy remains the most favorable option after surgical removal to eradicate breast tumor cells. Paclitaxel (PTX) is the first-line agent for breast cancer, especially for metastatic or HER2-negative breast cancer [13,14]. It possesses multiple anti-tumor activities [15]. The classical pharmacological activity of PTX is that it disrupts microtubule dynamics by promoting tubulin polymerization and stability as well as inducing apoptosis and cell cycle arrest in tumor cells [16,17]. Additionally, a variety of tumor-inhibitory effects of PTX through other mechanisms have recently been revealed [18–20]. For example, it has been found that PTX, with prolonged exposure time and metronomic schedules, may have anti-angiogenic properties [21]. Moreover, previous studies have clearly revealed that the efficacy of PTX in malignant cells is highly dose-dependent. It exerts diverse effects via specific mechanisms at different doses [22–25].

Apart from its tumor-suppressive effects, PTX in clinical concentration elicits a transient 'cytokine storm' in breast cancer patients [26,27]. The proinflammatory effect of PTX is dependent on Toll-like receptors (TLRs) signaling and has been proven to be the primary effect resulting in cancer treatment failure, tumor resistance or even induction of the lymph node and pulmonary metastasis of breast cancer [28,29]. However, the influence of PTX on other organ-targeted metastases of breast cancer and its direct regulation in the host organ, most importantly in the liver microenvironment, remains missing.

Pharmacokinetically, PTX was selectively enriched and metabolized in liver [30]. However, its metabolism and distribution features are highly individual. In addition, accompanying PTX metabolism and degradation *in vivo*, the effective PTX concentration dynamically decreases. Therefore, it is inevitable and non-negligible that the PTX concentration will be far lower than the clinical dose in tumor tissues, especially in the later phase of one medication cycle. Clinically, restricted by the severe cytotoxic effects, the 'low-dose metronomic' chemotherapeutic pattern is preferable for most Asian patients [31] and the medication cycle of PTX usually contains long dosing intervals. These lead to the increased opportunity for exposure or prolonged exposure time to low-dose PTX in cancer patients. Taking the dose-dependent feature of PTX efficacies into account, a detailed analysis of PTX efficacy at low dose and its relevance to tumor progression is necessary and will be beneficial for reasonable PTX application; however, such studies are still lacking.

Collectively, our study was designed to reveal how low-dose PTX regulates tumor disease progression and to identify the influence of low PTX on host organ microenvironment.

To complete our study, we compared the effects of PTX with the clinical dose (equivalent to 20 $mg{\cdot}kg^{-1}$ in mouse) or lower than the clinical achievable dose in breast tumor-bearing mouse models. Surprisingly, we found that low and high doses of PTX showed completely different efficacies. Low-dose PTX induced more liver metastasis, which greatly attracted our attention. Further study for the first time revealed that low-dose PTX, with little tumoricidal effect, functioned as a potent inducer for breast cancer progression in a nuclear factor-κB (NF-κB) -dependent manner. We also observed the expression changes of drug metabolic enzymes in host hepatocytes, which might result in the oncological rebuilding of the estrogen metabolic balance and the promoting of metastasis in the liver microenvironment. Our study provided experimental indications of how to avoid the side-effects and optimize the toxicity–efficacy ratio of PTX and will be beneficial for the reasonable application of PTX during cancer treatment.

Results

High and low doses of PTX show different efficacies on breast cancer cells

According to chemotherapeutic strategy, the clinically used dose of PTX is 90–200 $mg{\cdot}m^{-2}$, which is equivalent to 20–50 $mg{\cdot}kg^{-1}$ in mouse. To compare the effects of different doses of PTX on tumor progression *in vivo*, MDA-231 tumor-bearing mice were treated with low-dose (1 $mg{\cdot}kg^{-1}$) and high-dose (20 $mg{\cdot}kg^{-1}$) PTX. In contrast to the efficient restriction of primary tumor in the high-PTX group (Fig. 1A,B), liver metastases were obviously induced in the low-PTX group with little influence on primary tumor growth (Fig. 1A–D). Morphologically, a large number of 1–3 mm diameter, pale-colored, dotted or plaque-like metastases can be directly observed in liver samples

collected from the low-dose PTX group. Histologically, hemotoxylin and eosin staining also showed that the light-colored spotted metastases were dramatically increased in livers from the low-dose PTX-treated mice. In contrast, the metastasis was substantially reduced in the high-dose PTX group compared with the negative control (Fig. 1E). Of note, in the same animal model, low-dose PTX did not affect cancer cells metastasizing to lungs, one of the most susceptible organs for breast cancer metastasis (Fig. 1F).

Moreover, to dynamically and specifically characterize the results mentioned above, the high-invasive mouse breast cancer cell 4T1, which can spontaneously metastasize to lungs *in vivo*, was selected for a tumor model. It was further constructed to stably express luciferase (4T1-Luc), and a small animal imaging system was used to trace and quantify the influence of PTX on the progression of breast cancer *in vivo*. Consistent with the above results, images and quantification data (Fig. 2) clearly showed that high-dose PTX obviously inhibited the primary tumor growth, whereas such effects cannot be detected in the low-dose PTX group. The tumor weight and the total photon values showed no significant difference between negative control and the low-PTX-treated group, and

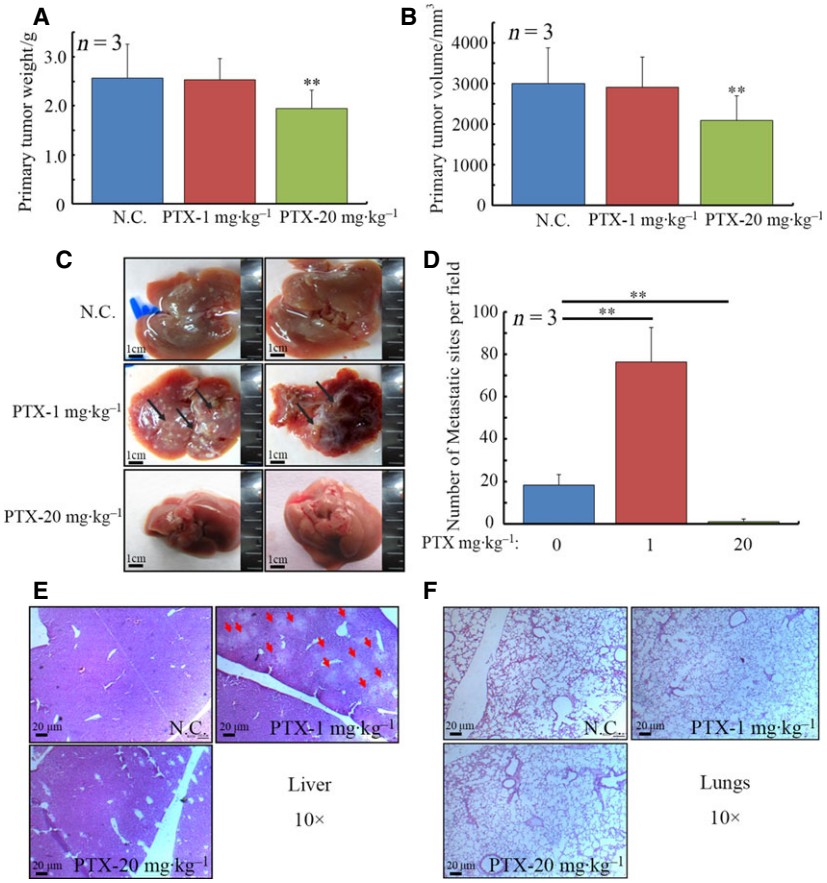

Fig. 1. The dose-determined effects of PTX on the metastasis of breast cancer *in vivo*. (A, B) Weight and volume analysis of primary tumor in MDA-231 xenograft-bearing mice. The high invasive breast cancer cells MDA-231 were transplanted in nude mice. After treating with indicated doses of PTX for five cycles (1 time/2 days), mice were euthanized, and the weight and volume of the primary tumor were quantified (N.C.: negative control; PTX-1 mg·kg^{-1} and PTX-20 mg·kg^{-1}: tumor-bearing mice treated with 1 and 20 mg·kg^{-1} PTX, respectively). The results demonstrated that low-dose PTX had little effect on the growth of primary breast tumors. (C, D) Morphological observation of livers. The number of metastases was further quantified. Mice livers were obtained on the 20th day after PTX treatment. The arrows indicate the metastatic sites. The result revealed the promoting effects of low-dose PTX on the formation of breast cancer liver metastases ($n = 3$ independent experiments). Scale bar: 1 cm. (E, F) Histological analysis of the livers and lungs in PTX-treated mice. Red arrows show the metastatic sites. The results showed that low-dose PTX induced liver metastasis *in vivo*, whereas it had no influence on metastasis to the lungs, which are also a common target for breast cancer metastasis. Scale bar: 20 μm. All the bar graphs show means ± standard deviation from three independent repeats. One-way analysis of variance (ANOVA) was used for all the quantifications: $^{**}P < 0.01$.

were about more than 2 times higher than those in the high-PTX group (Fig. 2A–C).

In contrast, the metastatic behavior was greatly influenced by low-dose PTX. In the later phase of tumor progression, the lung metastases can be clearly detected and their intensities kept at a similar level in the negative control and the low-PTX group. However, liver preferential metastasis can be obviously and specifically detected in response to low PTX. As expected, high PTX efficiently suppressed the metastatic colonization of breast cancer in all of the four susceptible organs (Fig. 2D,E). This result provided further evidence for the promotion effect of low PTX on the liver metastases of breast cancer.

Low-dose PTX induces the expression of genes mediating cancer-related inflammation in MDA-231 cells

To further reveal the underlying effects of low-dose PTX at the molecular level, gene microarray analysis was performed. In genome-wide screening and cluster analysis, the low-dose PTX responsive genes exhibited a typical proinflammatory signature (Fig. S1 and Fig. 3A, Table 1).

Subsequently, 100 $ng{\cdot}mL^{-1}$ clinical-dose PTX (for clinical use, the equivalent PTX concentration *in vitro* ranges from 85 to 2500 $ng{\cdot}mL^{-1}$ [25,32]) and ultra-low-dose PTX (less than 30 $ng{\cdot}mL^{-1}$) were used and the prediction from microarray analysis was identified *in vitro*. Firstly, we found that, consistent with the clinical-dose PTX, low-dose PTX also possessed potent activity to enhance the expression of inflammatory molecules in a wide-spectrum of tumor cells. These cell lines were originated from the malignancies that were the typical PTX-responsive tumors in clinical treatment, including breast cancer, lung cancer and ovarian cancer (Fig. 3B).

Furthermore, using MDA-231 as the model, detailed analysis identified that, with little alteration in cell survival (Fig. 3C), chemokines, cytokines and inflammatory adhesion molecules were all elevated at both the mRNA and the protein levels in low-dose PTX-treated cells. For example, low PTX induced more than 200-folded and 2000-folded transcriptional upregulation for interleukin (IL) 8 and chemokine (C-C motif) ligand 20 (CCL20), respectively. Accordingly, the secretion levels of IL8 and IL6 were about five times and three times higher, respectively, than negative control (Figs 3D–F and 4A–F).

The above molecular changes were also proved *in vivo*. In low-dose PTX-exposed tumor-bearing mice, the above-mentioned inflammatory cytokines or chemokines were all elevated systematically (Fig. 4G,H). In addition, low-dose PTX induced the expression of the inflammation adhesion molecules, including intercellular adhesion molecule 1 (ICAM-1) and vascular cell adhesion molecule 1 (VCAM-1), in primary tumor samples (Fig. 4I).

Low-dose PTX directly induces the epithelial–mesenchymal transition and functionally enhances breast tumor motility and invasion

In addition to the above findings, the detailed molecular analysis further indicated that, different from clinical-dose PTX, low-dose PTX not only resulted in similar proinflammatory and angiogenic responses in the host microenvironment as reported by Lisa Volk-Draper and colleagues [29], but also directly had a promalignant effect on tumor cells themselves. Under low-dose PTX treatment, the molecular expression change revealed a clear epithelial–mesenchymal transition (EMT) profile. E-cadherin, a well-known epithelial marker and potent metastatic inhibitor, was reduced. Conversely, the mesenchymal marker vimentin, the EMT mediator integrin β3 and the initiator Twist were all significantly upregulated in response to low PTX treatment (Fig. 5A). These changes were further identified in primary tumor samples obtained from an animal model (Fig. 5B). This suggested that the effects of PTX are highly dependent on its dose. At high concentration, due to the potent tumoricidal effect, PTX functions as a suppressor of tumor growth. In contrast, when dose decreases, the tumor toxic effect of PTX is largely weakened and only the promalignant effects can be predominantly detected.

Fig. 2. Low-dose PTX has little inhibitory effect and enhances the liver metastasis of breast cancer *in vivo*. To observe the disease progression in a broader range, 4T1-Luc cells were transplanted into Balb/C mice (10 mice per group) and designed to grow over a longer time compared with the model in Fig. 1. After regular PTX administration, the primary tumor images were collected (A) and their weights and total photon values were quantified (B, C). The result revealed that the tumor-inhibitory effect was largely weakened by the decrease of PTX dose. Scale bar: 1.8 cm. (D) Images of metastatic lesions in liver and lungs. Representative images are shown (three mice per group). Scale bar: 7 mm. (E) Total photon analysis for the target organs of breast cancer metastasis (liver, lungs, brain and bone). The result further identified the liver metastasis promoting effect of low-dose PTX. All the bar graphs show means ± standard deviation from three independent repeats. One-way ANOVA was used for all the quantifications: $*P < 0.05$, $**P < 0.01$, $***P < 0.001$.

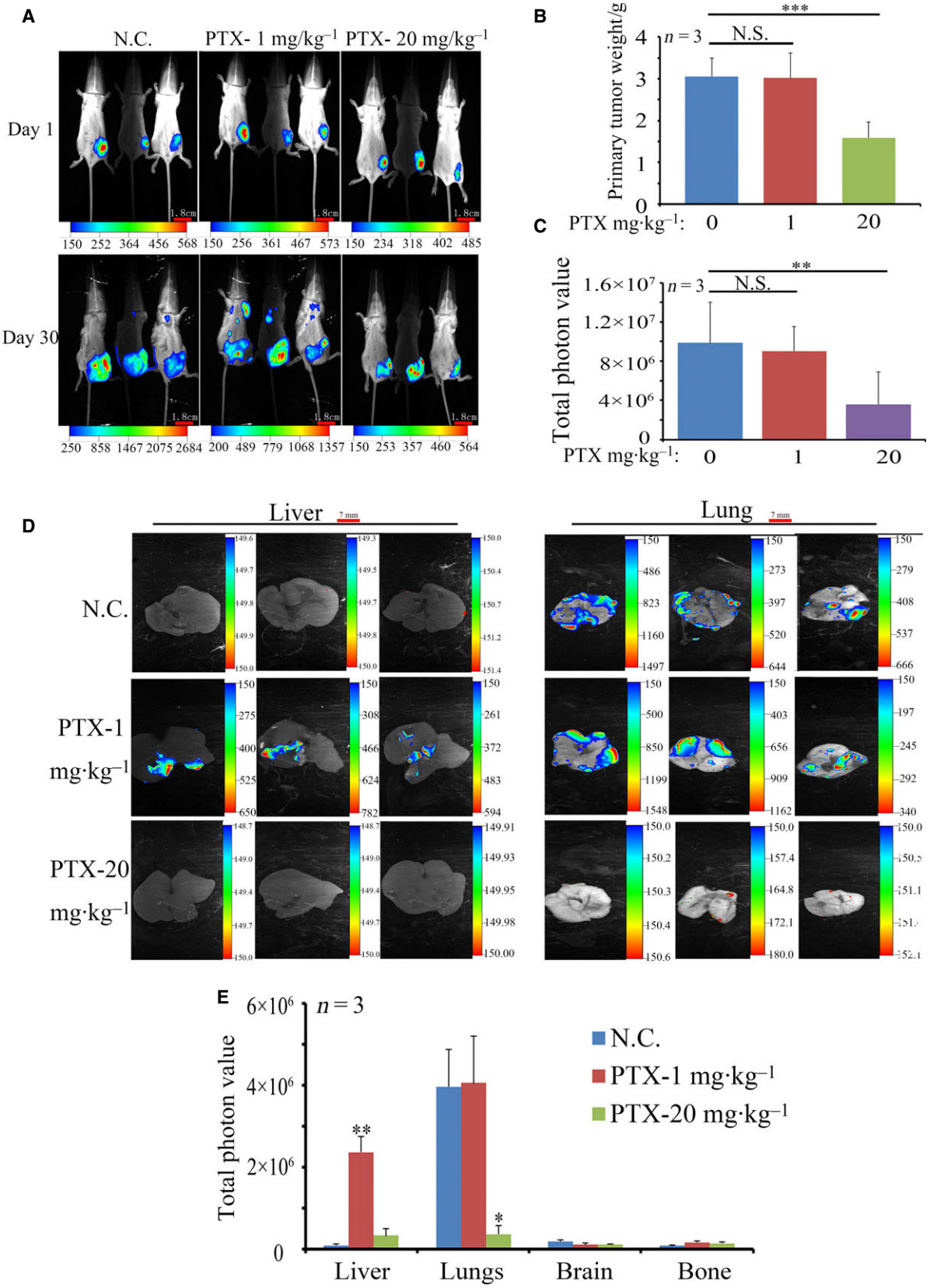
A
N.C.
PTX- 1 mg/kg⁻¹
PTX- 20 mg/kg⁻¹
Day 1
Day 30
B
Primary tumor weight/g
n = 3
N.S.
***
PTX mg·kg⁻¹: 0 1 20
C
Total photon value
n = 3
N.S.
**
PTX mg·kg⁻¹: 0 1 20
D
Liver
Lung
N.C.
PTX-1 mg·kg⁻¹
PTX-20 mg·kg⁻¹
E
Total photon value
n = 3
N.C.
PTX-1 mg·kg⁻¹
PTX-20 mg·kg⁻¹
Liver
Lungs
Brain
Bone

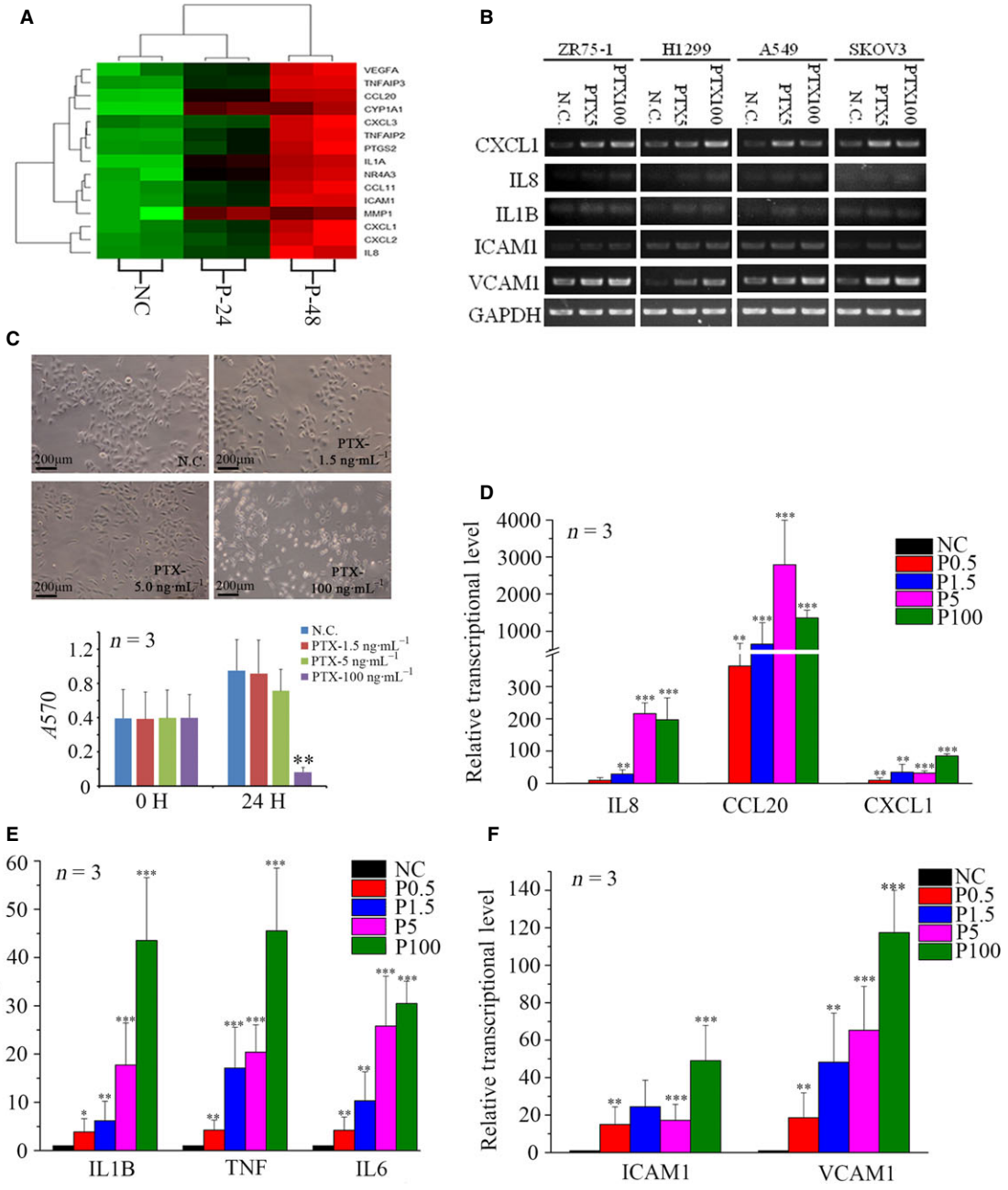

Fig. 3. Low-dose PTX transcriptionally upregulates the inflammatory molecules in MDA-231 cells. (A) Micro-array screening and clustering analysis of inflammatory molecule expression in MDA-231 cells. NC: negative control; P-24 and P-48: cells treated with low-dose PTX for 24 and 48 h, respectively. The results showed that inflammatory molecules were dramatically induced in response to low-dose PTX. (B) Low-dose PTX induced inflammatory responses in a wide range of cancer cells. Low-dose (5 ng·mL^{-1}) or clinical-dose (100 ng·mL^{-1}) PTX was used to treat breast (ZR75-1), lung (H1299, A549) and ovarian (SKOV3) cancer cells. The results showed that inflammatory factors and adhesion molecules were transcriptionally enhanced by low PTX. (C) Morphological observation (upper panel) and MTT quantification (lower panel) of low- and clinical-dose PTX-treated MDA-231 cells. Results revealed there was little influence of low-dose PTX on cell survival and growth. Scale bar: 200 μm. Imaging and MTT assay were performed 24 h after treatment. (D–F) Real-time PCR analysis in low-PTX-treated MDA-231 cells. Results showed that, compared with PTX-non-treated cells, the expressions of chemokines (IL8, CCL20, CXCL1), inflammatory cytokines (IL1B, TNF, IL6) and adhesion molecules (VCAM1 and ICAM1) were all obviously upregulated by low-dose PTX. All the quantitative data in (C–F) are means ± standard deviation from three independent repeats. One-way ANOVA was used for all the quantifications: $*P < 0.05$, $**P < 0.01$, $***P < 0.001$. CCL20, chemokine (C-C motif) ligand 20; CXCL1, chemokine (C-X-C motif) ligand 1; ICAM1, intercellular adhesion molecule 1; IL6, interleukin 6; IL8, interleukin 8; TNF, tumor necrosis factor; VCAM1, vascular cell adhesion molecule 1.

Table 1. GO and PATHWAY analysis for microarray screening in low-dose PTX-treated MDA-MB-231 cells. The GO and PATHWAY analysis was performed after the gene expression microarray data were obtained. For this analysis, the upregulated and downregulated fields are listed in the table.

Category	Term	Name	*P*-value	Bonferroni	Expression change
GO (BP)	GO:0009611	Response to wounding	7.65×10^{-6}	0.012177037	Upregulation
O (BP)	GO:0006955	Immune response	9.03×10^{-6}	0.014367332	Upregulation
GO (BP)	GO:0006954	Inflammatory response	1.77×10^{-5}	0.027992401	Upregulation
GO (BP)	GO:0051240	Positive regulation of multicellular organismal process	1.98×10^{-5}	0.031204768	Upregulation
GO (BP)	GO:0001666	Response to hypoxia	1.99×10^{-5}	0.031365568	Upregulation
GO (BP)	GO:0070482	Response to oxygen levels	2.98×10^{-5}	0.046683098	Upregulation
GO (CC)	GO:0005615	Extracellular space	2.43×10^{-6}	4.90×10^{-4}	Upregulation
GO (CC)	GO:0044421	Extracellular region part	4.35×10^{-5}	0.008746324	Upregulation
GO (MF)	GO:0005125	Cytokine activity	1.73×10^{-6}	5.36×10^{-4}	Upregulation
GO (MF)	GO:0008009	Chemokine activity	1.09×10^{-5}	0.003384946	Upregulation
GO (MF)	GO:0042379	Chemokine receptor binding	1.58×10^{-5}	0.004913466	Upregulation
KEGG_PATHWAY	hsa04621	NOD-like receptor signaling pathway	2.73×10^{-6}	2.68×10^{-4}	Upregulation
KEGG_PATHWAY	hsa05200	Pathways in cancer	2.50×10^{-4}	0.024211097	Upregulation
KEGG_PATHWAY	hsa04060	Cytokine–cytokine receptor interaction	3.87×10^{-4}	0.037229638	Upregulation
GOTERM_BP_FAT	GO:0006260	DNA replication	1.04×10^{-4}	0.04269147	Downregulation
GOTERM_BP_FAT	GO:0006281	DNA repair	2.31×10^{-8}	9.73×10^{-6}	Downregulation
GOTERM_BP_FAT	GO:0006974	Response to DNA damage stimulus	2.38×10^{-7}	1.00×10^{-4}	Downregulation
GOTERM_BP_FAT	GO:0033554	Cellular response to stress	7.57×10^{-6}	0.003180086	Downregulation
GOTERM_BP_FAT	GO:0006259	DNA metabolic process	2.86×10^{-7}	1.21×10^{-4}	Downregulation

To further investigate whether the molecular changes led to functional alterations of breast tumor cells, the Transwell cell migration assay was performed. By treating MDA-231 cells with 0.5 and 1.5 $ng \cdot mL^{-1}$ PTX, the transmembrane rate was significantly increased in the low-PTX groups (Fig. 5C). Moreover, in a cell detachment assay, an increased number of adherent cells were observed in a dose-dependent manner. In the negative control group, the trypsinized cells had a rounded morphology and were dissociated from the matrix, whereas cells treated with 5–15 $ng \cdot mL^{-1}$ PTX maintained a spindle cell shape. These results revealed that the cells were more resistant to trypsinization after PTX treatment, further demonstrating that PTX treatment promoted cell adhesion (Fig. 5D). Accordingly, actin polymerization was also obviously enhanced in low-PTX-treated MDA-231 cells, which suggested a promigration effect of low PTX in breast cancer cells (Fig. 5E).

To further mimic the process of tumor cell invasion and infiltration into surrounding tissue *in vitro*, the Matrigel cell invasion assay was performed. Figure 5F shows that the transmembrane rate was about three times higher than that in negative control cells. Notably, breast cancer cells respond specifically to low-dose PTX in the promotion of tumor invasiveness. High-dose PTX (100 $ng \cdot mL^{-1}$) failed to induce the same phenotypic changes as low-dose PTX. Its transmembrane cells were about 10 times lower than the low-dose PTX group. These results phenotypically supported the molecular alteration induced by low-dose PTX.

Activation of NF-κB is required for the oncological behaviors induced by low-dose PTX

Based on the central roles of NF-κB in the regulation of tumor-associated inflammation and cancer progression, we next examined the connection between low-dose PTX and NF-κB. In a dual-luciferase reporter gene assay, we found about 8-fold higher luminescence intensity in the low-PTX group compared with the control group, initially revealing that NF-κB was activated by low-dose PTX (Fig. 6A). Western blot analysis further confirmed the NF-κB activating effects of low-dose PTX on breast tumor cells from both *in vivo* and *in vitro* models. The phosphorylation levels of IκB kinase (IKK) and p65 were elevated, whereas the essential NF-κB inhibitor, IκB, was significantly downregulated in response to low PTX (Fig. 6B,C).

Additionally, by treatment with the NF-κB inhibitor BAY117082 (BAY), the inflammation-stimulating activity of low-dose PTX was largely inhibited (Fig. 6D). For instance, the transcriptional level of IL8 in PTX and BAY combined-treated cells was eight times lower than that in cells treated with PTX alone.

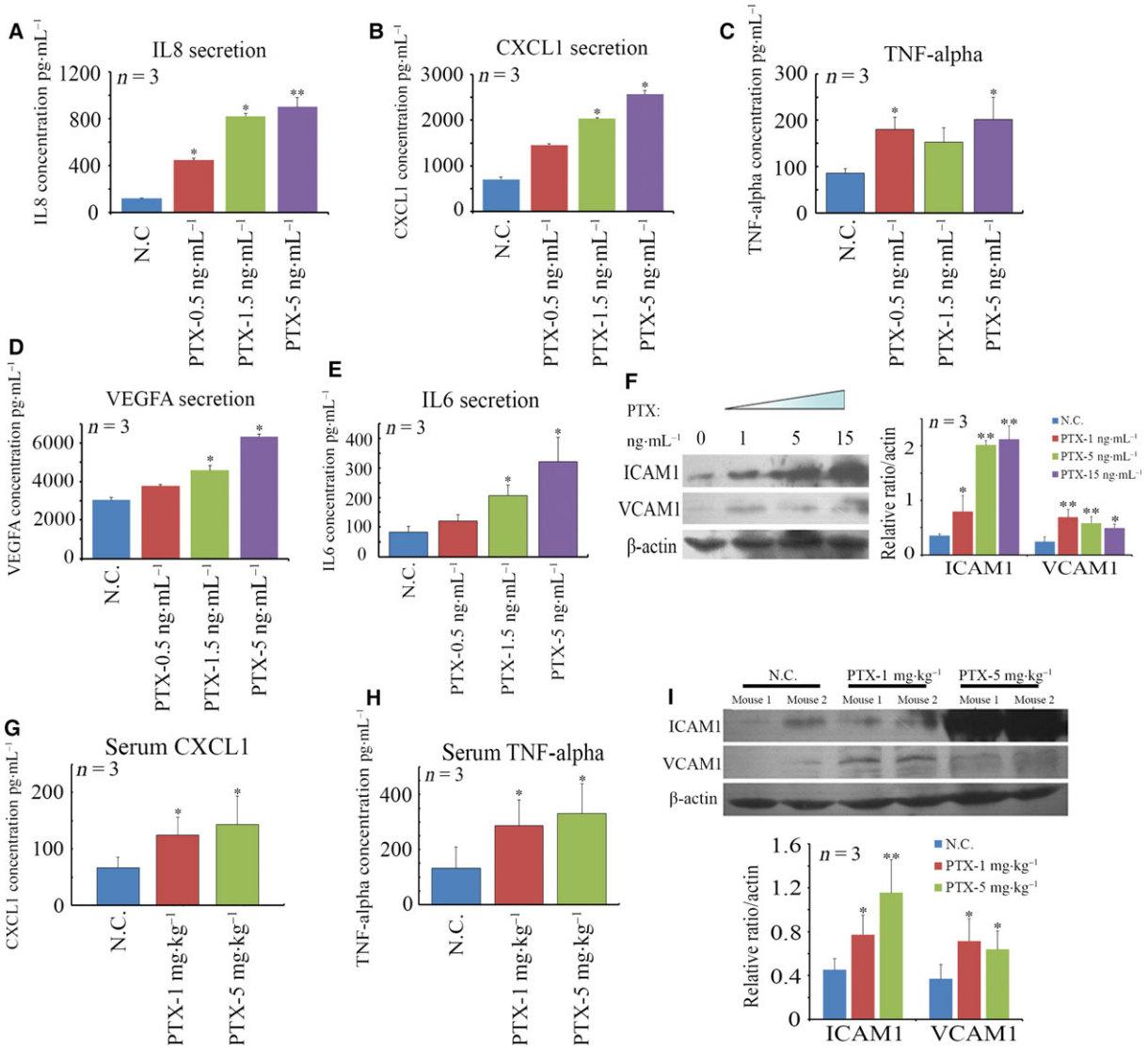

Fig. 4. Low-dose PTX induces the expression of inflammatory molecules in breast cancer cells. (A–E) ELISA identification of the secretion of inflammatory factors. Cultural supernatants were collected and analyzed 48 h after treatment. In accordance with the alterations at the mRNA level, the ELISA results demonstrated that the secretion of inflammatory molecules (including IL8, CXCL1, TNF-α, vascular endothelial growth factor A (VEGFA) and IL6) were consistently enhanced in response to low-dose PTX. (F) Western blot identification of adhesion molecules in low-PTX-treated MDA-231 cells. After the same treatment as described in (A), the expression of adhesion molecules was further analyzed. Results revealed the enhanced expression of VCAM1 and ICAM1 in the presence of low-dose PTX. The quantification of gray value for each band (comparing with its internal control) was statistically analyzed in the right bar graph. (G, H) ELISA detection of inflammatory factors in serum from tumor-bearing mice treated with low-dose PTX. Results revealed that the key factors mediating inflammation were systematically induced in low-PTX-exposed mice. (I) Western blot analysis of the adhesion molecules in primary tumors from low-PTX-treated tumor-bearing mice. Two mice primary tumor samples from each group were selected to detect the expression of adhesion molecules. Representative results from two mice in the same group (Mouse 1 and 2) are shown and the gray value of each sample compared with its internal control is statistically quantified below. These data further support the proinflammatory effects of low-dose PTX *in vivo*. The bar graphs show means ± standard deviation from three independent repeats. One-way ANOVA was used for all the quantifications: $*P < 0.05$, $**P < 0.01$.

Furthermore, consistent with the molecular changes, in a Transwell assay, the number of transmembrane cells in the combined treated group was 134, which was 4.3 times lower than that in the PTX-non-treated group (Fig. 6E). These results functionally suggest that NF-κB is responsible for the upregulated inflammation and the enhanced tumor motility induced by low-dose PTX.

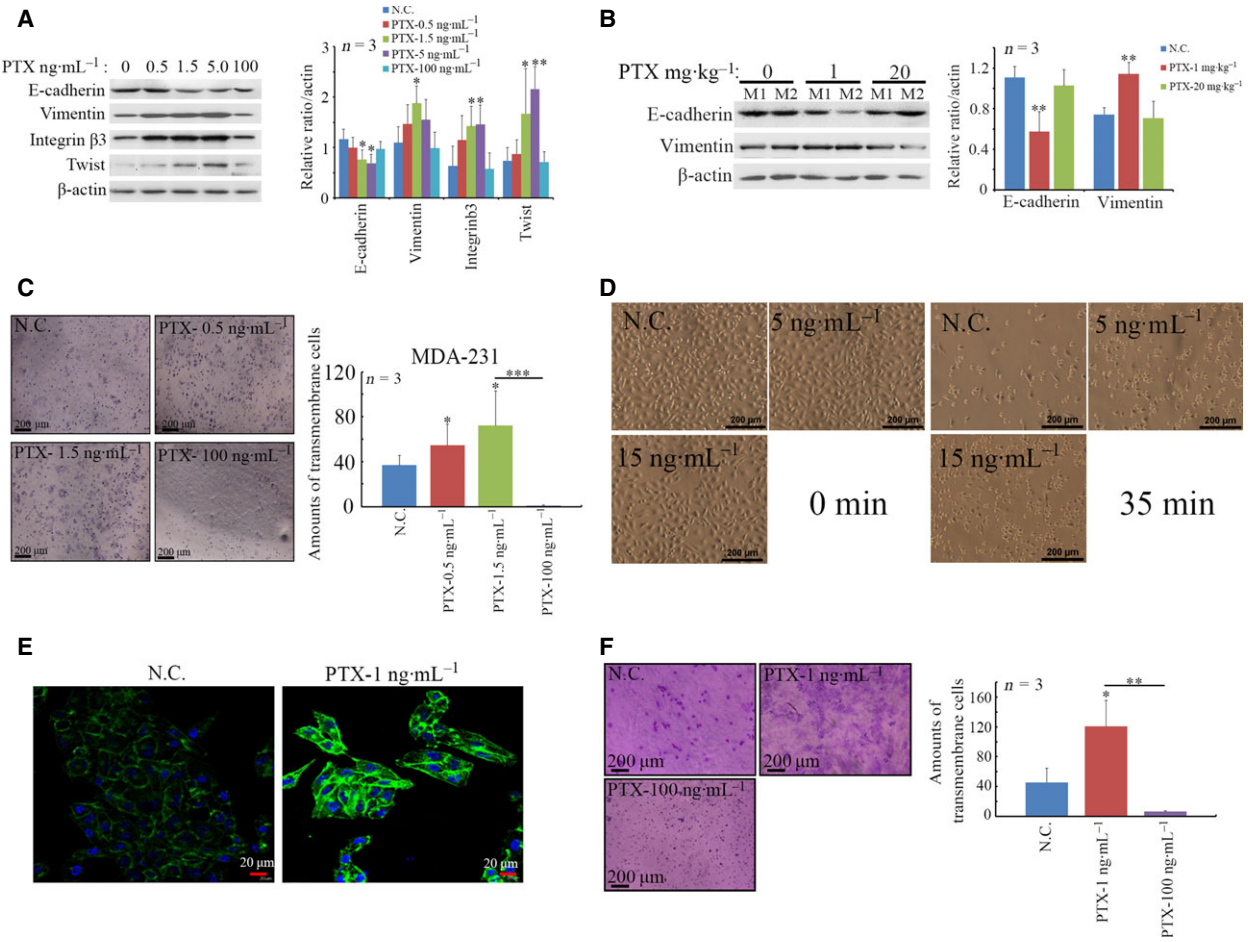

Fig. 5. Low-dose PTX induces epithelial–mesenchymal transition (EMT) and promotes cell migration and invasion in breast cancer cells. (A) Western blot analysis of the EMT molecular markers in MDA-231 cells treated with low PTX for 48 h. Gray value quantification comparing with internal control was further performed and statistically analyzed (as shown on the right). $n = 3$, $^{*}P < 0.05$, $^{**}P < 0.01$. (B) Western blot analysis of the EMT molecular markers in primary tumor samples mentioned in Fig. 2. The representative result obtained from two mice in the same group (M1 and M2) is shown and the gray value quantification for each sample was analyzed and shown on the right. Results molecularly demonstrated that low-dose PTX induced the typical EMT pattern in breast cancer cells. $n = 3$, $^{*}P < 0.05$, $^{**}P < 0.01$. (C) Transwell assay of MDA-231 treated with 0.5–1.5 ng·mL^{-1} (low-dose) PTX or 100 ng·mL^{-1} (high-dose) PTX. Scale bars, 200 μm.The transmembrane cells were further quantified. The result showed that, different from high-dose PTX, low-dose PTX enhanced the motility of MDA-231 cells. $^{*}P < 0.05$, $^{***}P < 0.001$. (D) Cell detachment assay for MDA-231 cells. Cells were treated with indicated doses of PTX for 24 h. Then, the cells were washed and trypsinized for 35 min with 0.00125% trypsin. Images were taken to assess the cell adhesion potential. The elevated resistance against trypsin was observed in low-PTX-treated cells. Scale bars, 200 μm. (E) Confocal microscopic observation of F-actin by phalloidin staining after low-PTX treatment for 36 h. The results demonstrated the enhanced polymerization and relocalization of F-actin in PTX-treated cells. Scale bars, 20 μm. (F) Matrigel invasive assay in low-PTX-treated EMT6 cells. The transmembrane cells were further quantified. $^{*}P < 0.05$, $^{**}P < 0.01$. Error bars represent the standard deviation. Scale bars, 200 μm. The results proved that low PTX induced increased matrix-degradation potential. One-way ANOVA was used for all the quantifications.

Low-dose PTX induces changes in estrogen metabolism in liver that facilitate the formation of breast cancer metastases

Next, we attended to the mechanism of the liver metastatic preference induced by low-dose PTX. In this study, we noticed that PTX is selectively enriched and metabolized in liver [30,33]. Led by this, we found that two PTX-related metabolic enzymes [34,35], cytochrome P450 1B1 (CYP1B1) and Cytochrome P450 3A4 (CYP3A4), were significantly induced in low-dose PTX-treated HepG2 cells (Fig. 7A,B). The transcriptional intensity of CYP1B1 was four times higher in low-PTX-treated cells. Interestingly, recent studies clearly showed that CYP1B1 was the risk factor involved in chemotherapy resistance in breast cancer

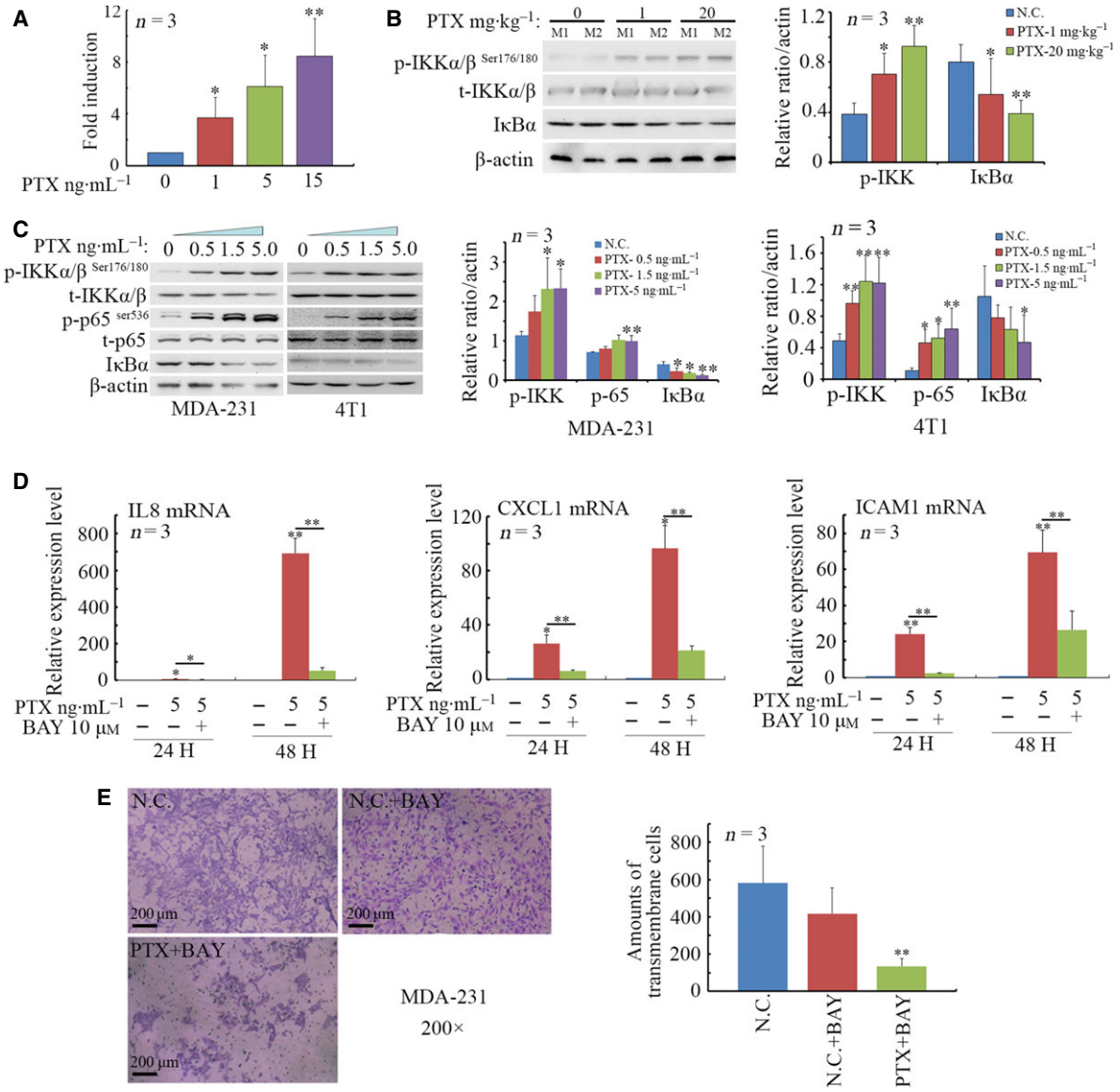

Fig. 6. Low-dose PTX functions as the promalignant factor in an NF-κB-dependent manner. (A) Dual luciferase reporter assay. Luciferase transfected cells were treated with the indicated doses of PTX for 24 h and the fluorescence was measured for NF-κB activation. Results identified the dose-dependent effects of PTX on the activation of NF-κB. (B) Western blot analysis of NF-κB key regulators in primary tumor samples obtained from Fig. 2. A representative result is shown (using two mice samples in each group: M1 and M2) and gray value quantification was further performed (the bar graph on the right). (C) Detection of NF-κB activation under low-dose PTX treatment in MDA-231 cells and 4T1 cells. The indicated doses of PTX were utilized and the cell lysates were prepared 2 h after treatment. The gray value for each band (comparing with internal control) was quantified and is shown on the right. The result showed that the key regulators of NF-κB were obviously influenced by low PTX, which further supported the stimulatory effects of PTX on this pathway. (D) Real-time RT-PCR of key inflammatory molecules in response to low-dose PTX treatment in the presence of the NF-κB-specific inhibitor BAY117082. The results showed that BAY117082 largely reversed the upregulation of inflammatory molecules induced by PTX. (E) Transwell assay in PTX and BAY combined-treated MDA-231 cells. The transmembrane cells were further quantified. The result proved that NF-κB activation is required for the enhanced cell motility induced by low PTX. Scale bar, 200 μm. All the quantitative data are collected from three independent repeats and represented by means ± standard deviation. One-way ANOVA was used for all the quantifications: $*P < 0.05$, $**P < 0.01$.

patients [35] and functionally participated in the oncological metabolism of the carcinogen 4-hydroxyestradiol (4-OHE2), which enhances malignancy of multiple cancer cells in both an estrogen-dependent and -independent manner [36–38]. Led by this, the above mRNA alteration was further identified in

tumor-free mice injected with 1 mg·kg^{-1} PTX for three courses of treatment intraperitoneally. The result showed that the CYP1B1 expression level was course-dependently upregulated (Fig. 7C). To the contrary, catechol-O-methyltransferase (COMT), the enzyme responsible for the detoxification of 4-OHE2 into methoxy derivatives [39], was obviously reduced in PTX-treated liver samples (Fig. 7D,E). Collectively, our results provided dual support, by selective enrichment in the liver, for low PTX resulting in the dysregulated expression of estrogen metabolic enzymes, which might contribute to the oncological shift of estrogen metabolism.

Discussion

PTX and its analogous compounds are the first line agents widely used in clinical cancer chemotherapy. However, potential risks and reasonable treatment strategies of PTX continue to be widely investigated [28].

Based on our study, we firstly observed that, specifically responding to low-dose PTX, metastases in liver colonized with much higher intensity than that in the negative control or the high-PTX group. We next revealed that the low and clinical doses of PTX have similar effects on the regulation of cancer-related

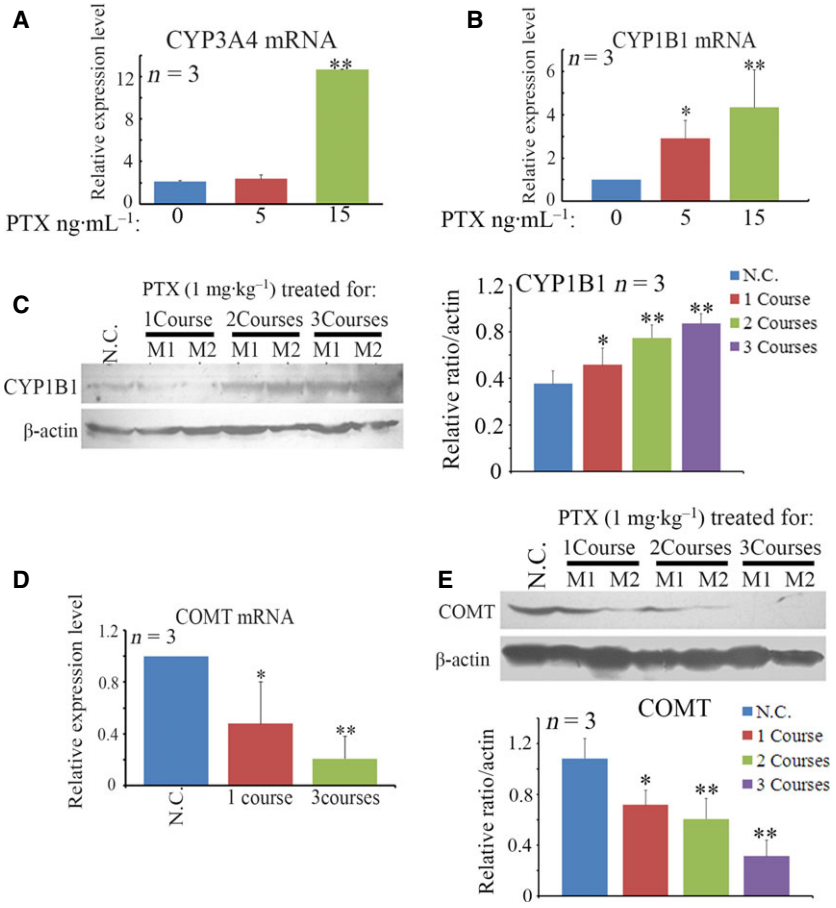

Fig. 7. Low-dose PTX induces carcinogenic estrogen metabolism in liver. (A, B) Real-time PCR analysis of the PTX-specific metabolic enzyme expression in low-dose PTX-treated HepG2 cells for 48 h. (C) Detection of CYP1B1 expression from mouse liver tissues. Tumor-free mice were treated with 1 mg·kg^{-1} PTX for three courses. A representative result is shown (two mice per group) and the relative gray value of each band compared with its internal control was statistically analyzed (shown on the right). The above results indicated that the metabolic enzymes (CYP1B1 and CYP3A4) were greatly induced in low-PTX-treated liver tissues. (D, E) Real-time RT-PCR and western blot analysis of COMT expression in liver from low-PTX-treated tumor-free mice referred to in (C). A representative result from two mice in the same group is shown and the relative gray value of each band compared with its internal control was statistically analyzed (shown below). The results indicated low PTX induced the procarcinogenic gene expression profile for estrogen metabolism. The histograms show means ± standard deviation collected from three independent experiments. One-way ANOVA was used for all the quantifications: $^{*}P < 0.05$, $^{**}P < 0.01$.

inflammation. In contrast, with little tumor-killing effect, the low-dose PTX-responsive genes have been well proven to extensively participate in tumor progression [40–43]. For instance, our study revealed that low-dose PTX induced more than 2000-fold upregulation of CCL20, which has been identified as the potent promalignant factor in breast cancer [44,45]. More importantly, in clinical survey, this gene expression pattern shares similarities with that of patients with inflammatory breast cancers. Many of the genes (COX2 or CXCL1) are further confirmed to be the core pathogenic factors for inflammatory breast cancers, which is highly consistent with our results [46].

Noteworthy, different from high-dose PTX, low-dose PTX not only molecularly induced the inflammatory response, but also functionally supported the tumor cell motility and invasive potential through the induction of EMT, which cannot be observed in the clinical-dose group. The transmembrane rate in the low-PTX-treated group was 2.7 times higher than that in the negative control. Based on such evidence, we have reason to note that, in addition to the similar efficacies in inflammatory promotion, low-dose PTX can directly potentiate tumor malignancy.

From the above results, we postulated that PTX has conflicting but highly correlated activities on malignancies: immune regulation and tumor cytotoxicity. The efficacy output for PTX is determined by its functional balance and our study clearly revealed that this balance is highly regulated by its dose. At clinically high dose, it exerts predominantly tumor-killing efficacy and efficiently blocks the progression of malignancies. Conversely, at the low concentration, PTX fails to function as the tumor suppressor but retains the potential to activate the NF-κB pathway. This leads to the rebalance of PTX efficacies, primarily inducing the repolarization of tumor cells and the reconstruction of the host microenvironment, which are both considered to be the main mechanism forcing tumor metastasis.

In addition to strengthened metastatic potential, we further obtained some indicative insights into the regulation of the hepatic microenvironment by PTX. It is well proven that PTX is selectively enriched in liver, and hepatic metabolism is the main elimination pathway for PTX [33]. In our studies, we found that low-dose PTX induced expression changes of drug metabolic enzymes (CYP1B1 and CYP3A4) in liver from tumor-free mice. In addition to their PTX metabolic activity [34,47], these enzymes are responsible for the hydroxylation of estrogens and activation of potential carcinogens in an estrogen receptor-independent mechanism [36,37]. CYP1B1 is the core

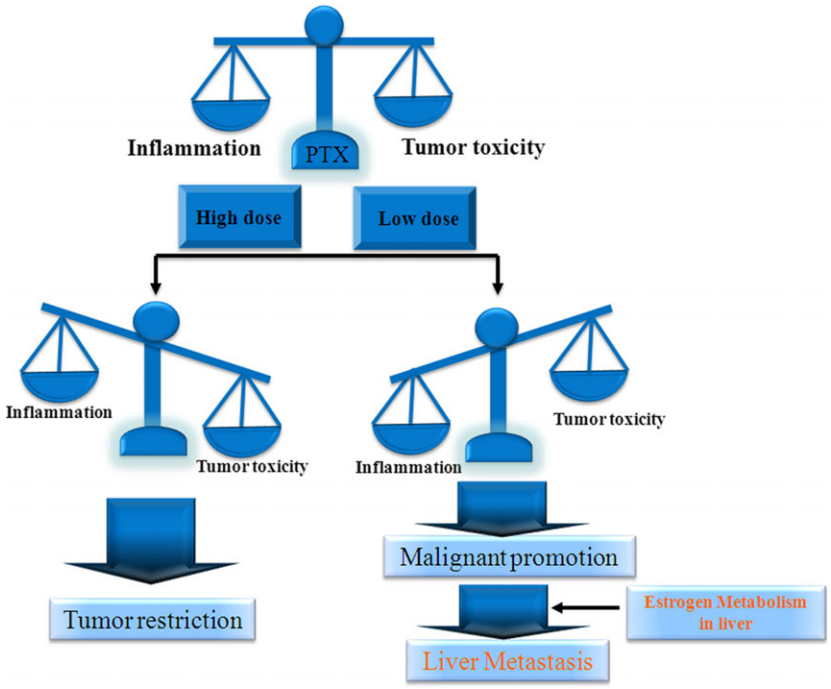

Fig. 8. Brief summary of the prometastatic effect of low-dose PTX in liver. The re-established balance for low-dose PTX stimulates cancer-related inflammation (CRI) and oncologically promotes the malignancy. In addition, by being selectively enriched and detoxified in liver, low-dose PTX might induce a functional shift in estrogen metabolism and facilitate the formation of metastases in liver.

mediator during estrogen receptor-independent carcinogenesis via activation of potential pathogenic factors [48]. Moreover, through catalysis of estrogen to 4-hydroxyestrogens, CYP1B1 is responsible for the activation of the invasive potential in human endometrial carcinomas [49]. Additionally, low-dose PTX also significantly and negatively influenced the expression of COMT, the major detoxifying enzyme for 4-hydroxyestrogens [39]. Collectively, we hypothesized that low-dose PTX can induce the dysregulated expression of estrogen metabolic enzymes and might provide a tumor-promoting microenvironment that facilitates the formation of metastases in liver.

In conclusion, in both immune-deficient and intact animal models, our findings proved that low-dose PTX enhanced liver-preferential metastasis and this phenomenon was determined by the synergistic integration of promalignant effects on breast tumor cells and the carcinogenic metabolism of estrogen in the liver microenvironment (Fig. 8). In light of the existing evidence, we can naturally extrapolate that low-level PTX, resulting from metabolic processes, drug distribution differences or individual variation, not only invalidates the clinical treatment, but also represents a risk factor that will lead to the promotion of malignancy and treatment failure. Notably, in current strategies for clinical therapy, a comprehensive and combined treatment is widely used in breast cancer. By the integration and complementation of different drug efficacies, the lowering of PTX dose with the aim of reducing toxic side-effects is adopted by most clinicians and believed to be beneficial for therapy optimization. In contrast with this belief, the results of our study alert us that such a strategy may have unexpected side-effects and should be carefully considered.

Due to the drug interaction and interference of efficacies in a combined cancer therapy strategy, more unstable factors were involved in the process of clinical data analysis and this largely limits the case selection and efficacy evaluation for low PTX. To further reveal the efficacy of PTX in patients, there is a need for the accumulation of more cases and a broader range of long-term statistical surveys in future studies.

Taken together, our study indicates that avoiding long-term exposure to low-dose PTX, by optimization of the medication strategy and combining the PTX treatment with a regulator of liver drug metabolic enzymes, may be beneficial and feasible for the reasonable application of clinical breast cancer chemotherapy.

Materials and methods

Reagents and cell culture

PTX injection solution was purchased from Union Pharmaceutical Factory (Beijing, China). The original PTX concentration was 6 $mg{\cdot}mL^{-1}$ in the solvent consisting of citric acid anhydrous, polyoxylethylene castor oil ether-35 and ethyl alcohol absolute. The PTX solution was further diluted to the indicated concentrations before use. Primary antibodies against Twist, vimentin, E-cadherin and p-IKK were purchased from Cell Signaling Technology (Danvers, MA, USA). In western blot analysis, they were diluted by a 5% BSA solution in Tris-buffered saline with Tween 20 (TBST) with the ratio of 1 : 1000. t-p65, p-p65, ICAM1, actin and CYP1B1 were purchased from Santa Cruz Biotechnology, Inc. (Dallas, TX, USA), and a 1 : 500 dilution was chosen for western blot analysis. Primary antibodies to t-IKK and IκB-α were purchased from Boster Bio-technology (WuHan, China) (dilution: 1 : 500). DAPI and phalloidin labelled with FITC were purchased from Sigma-Aldrich (St. Louis, MO, USA). Human IL8, VEGFA, TNF-α and IL6 and murine TNF-α ELISA kit were purchased from Dakewei Bioengineering Co. Ltd (Shenzhen, China); human CXCL1 was purchased from Cusabio Biotech Co. Ltd (Wuhan, China).

The breast cancer cell lines MDA-MB-231 (named MDA-231 for short), ZR75-1 and 4T1, lung cancer cell lines H1299 and A549 and the ovarian cancer cell line SKOV3 were purchased from the American Type Culture Collection (Manassas, VA, USA) and cultured with RPMI-1640 or Dulbecco's modified Eagle's medium (DMEM) supplemented with 10% fetal bovine serum (FBS) and 1% penicillin/streptomycin in a humid incubator with 5% CO_2.

Primary tumor growth and metastasis detection *in vivo*

Specific pathogen free (SPF) nude mice were purchased from the Vital River Laboratory Animal Technology Co. Ltd (Beijing, China). MDA-231 cells (1×10^6) were subcutaneously transplanted. After the formation of primary tumors (diameter > 5 mm), the mice were randomly grouped (10 mice per group) and different doses of PTX were diluted with normal saline and administrated by intraperitoneal injection (1 time/2 days). After five cycles of treatment, the mice were euthanized. The primary tumor growth and metastatic intensities were then measured, and images were captured. The procedures of animal experiments mentioned in our study were approved by the Animal Care and Welfare Committee of Peking University Health Science Centre. The animal housing facility was in accordance with the guidelines of the national standard *Laboratory Animals—Requirements of Environment and Housing Facilities (GB 14925–2001)*. The care of the laboratory animals and the experimental operations were

carried out in accordance with the *Regulations for the Administration of Laboratory Animals*.

Small-animal imaging assay

Metastatic 4T1 cells with stable firefly luciferase expression were provided by Caliper Life Sciences (Hopkinton, MA, USA). In this assay, 1×10^5 cells were resuspended in sterile PBS and subcutaneously injected into the inguinal area of 8-week-old female Balb/C mice. The tumor-bearing mice were randomly grouped (10 mice per group) after the formation of the primary tumor (about 10 days). Subsequently, the mice were intraperitoneally injected with PTX (1 time/2 days) to the end of the experiment. On the 40th day after drug administration, animals were sacrificed and the primary tumors, breast cancer preferential metastatic organs, including lungs, liver, brain and bones, were imaged and prepared for further analysis. All procedures were conducted in accordance with the China Experimental Animal Ethics Committee.

The primary tumor growth and the pulmonary metastatic behaviors were dynamically visualized and quantified with the Image Station System (Kodak, Rochester, NY, USA). Before detection, 200 μl firefly D-luciferin potassium salt (reconstituted in sterile PBS to the concentration of 15 $mg{\cdot}mL^{-1}$), which is the substrate for luciferase, was applied by hypodermic injection. After reaction for 10 min, the mice were anaesthetized by isoflurane and imaged.

Gene microarray analysis

For genome-wide gene expression analysis, MDA-231 cells were treated with 5 $ng{\cdot}mL^{-1}$ PTX for 24 and 48 h and then cell lysates were prepared with TRIzol reagent. Then the total RNA in each group was extracted and the genome-wide gene expressing profile was obtained with the Human One Array (HOA) microarray system (Phalanx Biotech Group, Hsinchu, Taiwan). The expression information was statistically analyzed using the Rosetta Resolver databases and the targeted genes were screened by its *P*-value calculated by the *t*-test by comparing each probe's normalized intensities and the negative control probe's intensity. If the *P*-value was lower than the threshold ($P < 0.05$), it indicates the gene expression was significantly different compared with the negative control. The differential genes were further analyzed by cluster analysis.

Transwell cell migration assay

The cells were starved overnight and 1×10^5 cells were seeded into the upper chamber of a Transwell insert (8 μm pore size; BD Falcon, San Jose, CA, USA) containing serum-free medium. The medium (containing 10% FBS) was placed into the lower chambers. After culturing for 24 h, the cells on the top surface of the membrane were gently swabbed and the transmembrane cells were fixed with 4% paraformaldehyde and stained with crystal violet (0.1% in ethanol). The cell motility was further quantified by cell counting in five randomly selected fields by microscopy (×200).

RT-PCR analysis

The cell lysates (1×10^6) were prepared with TRIzol reagent (Thermo Fisher Scientific, Waltham, MA, USA), and the total mRNA was extracted according to the manufacturer's instructions. Then, the total mRNA (1 μg) was digested with DNaseI at 37°C for 30 min and further reverse-transcribed using the RevertAid First Strand cDNA Synthesis Kit (Fermentas, Burlington, ON, Canada). The protocol for cDNA synthesis was as follows: 45 °C for 1 h followed by 70 °C for 5 min. Then, the gene transcription intensity was detected by real-time PCR (ABI 7500 system, Thermo Fisher Scientific) by utilizing the primers described in Table S1.

Cell detachment assay

Briefly, breast cancer cells (1×10^6) were treated with different concentrations of PTX and cultured for 24 h. Then, the cells were digested for a maximum of 40 min with 0.005% trypsin in Mg^{2+}/Ca^{2+}-free PBS. The trypsinized cells were imaged at the indicated time points. The cellular adhesion strength was assayed by determining the relative sensitivity to trypsin.

Statistical analysis

The results are expressed as the arithmetic mean ± standard deviation. All experiments were repeated at least three times and statistically analyzed by using IBM SPSS STATISTICS v. 19.0 (IBM, Armonk, NY, USA). One-way analysis of variance (one-way ANOVA) with least significant difference (LSD) or Tukey's *post hoc* test was used for all the quantifications ($*P < 0.05$; $**P < 0.01$, $***P < 0.001$).

Acknowledgements

This work is supported by grants from the National Natural Science Foundation of China (91129707, 81172001 and 81303272).

Conflicts of interest

The authors declare no potential conflicts interests.

Author contributions

QL, ZM and BS evaluated and performed the functional experiments *in vitro* and *in vivo*. QL, YLiu, XK and YLi recorded, analyzed and interpret the

experimental data. YZ, PW and QL were in charge of the analysis and interpretation of microarray data. QL, YLuo and DN participated in the mechanism analysis and performed the molecular detection both *in vitro* and *in vivo*. QL, LW and GZ wrote the manuscript and drafted the illustrations. LW and XZ designed the experiment and gave final approval of the version to be published. All the authors have read the manuscript and approved this version to be finally submitted.

References

1 Vulcano E, Montesano M, Battista C, Carino R, Perrone G, Vincenzi B & Altomare V (2010) Urinary complications from breast cancer metastasis: case report and review of the literature. *G Chir* **31**, 243–245.

2 Are C, Simms N, Rajput A & Brattain M (2010) The role of transforming growth factor-beta in suppression of hepatic metastasis from colon cancer. *HPB (Oxford)* **12**, 498–506.

3 Drasin DJ, Robin TP & Ford HL (2011) Breast cancer epithelial-to-mesenchymal transition: examining the functional consequences of plasticity. *Breast Cancer Res* **13**, 226.

4 Kang Y, Siegel PM, Shu W, Drobnjak M, Kakonen SM, Cordon-Cardo C, Guise TA & Massague J (2003) A multigenic program mediating breast cancer metastasis to bone. *Cancer Cell* **3**, 537–549.

5 Fidler IJ (2002) Critical determinants of metastasis. *Semin Cancer Biol* **12**, 89–96.

6 Fidler IJ & Kripke ML (1977) Metastasis results from preexisting variant cells within a malignant tumor. *Science* **197**, 893–895.

7 Bos PD, Zhang XH, Nadal C, Shu W, Gomis RR, Nguyen DX, Minn AJ, van de Vijver MJ, Gerald WL, Foekens JA *et al.* (2009) Genes that mediate breast cancer metastasis to the brain. *Nature* **459**, 1005–1009.

8 Minn AJ, Gupta GP, Siegel PM, Bos PD, Shu W, Giri DD, Viale A, Olshen AB, Gerald WL & Massague J (2005) Genes that mediate breast cancer metastasis to lung. *Nature* **436**, 518–524.

9 Berman AT, Thukral AD, Hwang WT, Solin LJ & Vapiwala N (2013) Incidence and patterns of distant metastases for patients with early-stage breast cancer after breast conservation treatment. *Clin Breast Cancer* **13**, 88–94.

10 Elias D, Lasser P, Spielmann M, May-Levin F, el Malt O, Thomas H & Mouriesse H (1991) Surgical and chemotherapeutic treatment of hepatic metastases from carcinoma of the breast. *Surg Gynecol Obstet* **172**, 461–464.

11 Bacalbasa N, Balescu I, Dima S & Popescu I (2015) Long-term survivors after liver resection for breast cancer liver metastases. *Anticancer Res* **35**, 6913–6917.

12 Selzner M, Morse MA, Vredenburgh JJ, Meyers WC & Clavien PA (2000) Liver metastases from breast cancer: long-term survival after curative resection. *Surgery* **127**, 383–389.

13 Yardley DA, Bosserman LD, O'Shaughnessy JA, Harwin WN, Morgan SK, Priego VM, Peacock NW, Bass JD, Burris HA III & Hainsworth JD (2015) Paclitaxel, bevacizumab, and everolimus/placebo as first-line treatment for patients with metastatic HER2-negative breast cancer: a randomized placebo-controlled phase II trial of the Sarah Cannon Research Institute. *Breast Cancer Res Treat* **154**, 89–97.

14 Einbeigi Z, Bergstrom D, Hatschek T & Malmberg M (2008) Paclitaxel, epirubicin and capecitabine (TEX) as first-line treatment for metastatic breast cancer: a pilot phase I/II feasibility study. *Clin Med Oncol* **2**, 533–538.

15 Rowinsky EK & Donehower RC (1995) Paclitaxel (taxol). *N Engl J Med* **332**, 1004–1014.

16 Bange J, Zwick E & Ullrich A (2001) Molecular targets for breast cancer therapy and prevention. *Nat Med* **7**, 548–552.

17 Pucci B, Bellincampi L, Tafani M, Masciullo V, Melino G & Giordano A (1999) Paclitaxel induces apoptosis in Saos-2 cells with CD95L upregulation and Bcl-2 phosphorylation. *Exp Cell Res* **252**, 134–143.

18 Pan Z, Avila A & Gollahon L (2014) Paclitaxel induces apoptosis in breast cancer cells through different calcium-regulating mechanisms depending on external calcium conditions. *Int J Mol Sci* **15**, 2672–2694.

19 Lu PH, Yu CC, Chiang PC, Chen YC, Ho YF, Kung FL & Guh JH (2011) Paclitaxel induces apoptosis through activation of nuclear protein kinase C-delta and subsequent activation of Golgi associated Cdk1 in human hormone refractory prostate cancer. *J Urol* **186**, 2434–2441.

20 Reshkin SJ, Bellizzi A, Cardone RA, Tommasino M, Casavola V & Paradiso A (2003) Paclitaxel induces apoptosis via protein kinase A- and p38 mitogen-activated protein-dependent inhibition of the Na^+/H^+ exchanger (NHE) NHE isoform 1 in human breast cancer cells. *Clin Cancer Res* **9**, 2366–2373.

21 Dumontet C & Jordan MA (2010) Microtubule-binding agents: a dynamic field of cancer therapeutics. *Nat Rev Drug Discov* **9**, 790–803.

22 Lu Z, Jia J, Di L, Song G, Yuan Y, Ma B, Yu J, Zhu Y, Wang X, Zhou X *et al.* (2011) DNA methyltransferase inhibitor CDA-2 synergizes with high-dose thiotepa and paclitaxel in killing breast cancer stem cells. *Front Biosci (Elite Ed)* **3**, 240–249.

23 Perera PY, Mayadas TN, Takeuchi O, Akira S, Zaks-Zilberman M, Goyert SM & Vogel SN (2001) CD11b/CD18 acts in concert with CD14 and Toll-like receptor

(TLR) 4 to elicit full lipopolysaccharide and taxol-inducible gene expression. *J Immunol* **166**, 574–581.
24 Kawasaki K, Gomi K, Kawai Y, Shiozaki M & Nishijima M (2003) Molecular basis for lipopolysaccharide mimetic action of Taxol and flavolipin. *J Endotoxin Res* **9**, 301–307.
25 Wang TH, Chan YH, Chen CW, Kung WH, Lee YS, Wang ST, Chang TC & Wang HS (2006) Paclitaxel (Taxol) upregulates expression of functional interleukin-6 in human ovarian cancer cells through multiple signaling pathways. *Oncogene* **25**, 4857–4866.
26 Zaks-Zilberman M, Zaks TZ & Vogel SN (2001) Induction of proinflammatory and chemokine genes by lipopolysaccharide and paclitaxel (Taxol) in murine and human breast cancer cell lines. *Cytokine* **15**, 156–165.
27 Pusztai L, Mendoza TR, Reuben JM, Martinez MM, Willey JS, Lara J, Syed A, Fritsche HA, Bruera E, Booser D *et al.* (2004) Changes in plasma levels of inflammatory cytokines in response to paclitaxel chemotherapy. *Cytokine* **25**, 94–102.
28 Rajput S, Volk-Draper LD & Ran S (2013) TLR4 is a novel determinant of the response to paclitaxel in breast cancer. *Mol Cancer Ther* **12**, 1676–1687.
29 Volk-Draper L, Hall K, Griggs C, Rajput S, Kohio P, DeNardo D & Ran S (2014) Paclitaxel therapy promotes breast cancer metastasis in a TLR4-dependent manner. *Cancer Res* **74**, 5421–5434.
30 Gustafson DL, Long ME, Bradshaw EL, Merz AL & Kerzic PJ (2005) P450 induction alters paclitaxel pharmacokinetics and tissue distribution with multiple dosing. *Cancer Chemother Pharmacol* **56**, 248–254.
31 Lien K, Georgsdottir S, Sivanathan L, Chan K & Emmenegger U (2013) Low-dose metronomic chemotherapy: a systematic literature analysis. *Eur J Cancer* **49**, 3387–3395.
32 Blagosklonny MV & Fojo T (1999) Molecular effects of paclitaxel: myths and reality (a critical review). *Int J Cancer* **83**, 151–156.
33 Panday VR, Huizing MT, Willemse PH, De Graeff A, ten Bokkel Huinink WW, Vermorken JB & Beijnen JH (1997) Hepatic metabolism of paclitaxel and its impact in patients with altered hepatic function. *Semin Oncol* **24**, S11-34–S11-38.
34 Taniguchi R, Kumai T, Matsumoto N, Watanabe M, Kamio K, Suzuki S & Kobayashi S (2005) Utilization of human liver microsomes to explain individual differences in paclitaxel metabolism by CYP2C8 and CYP3A4. *J Pharmacol Sci* **97**, 83–90.
35 De Iuliis F, Salerno G, Taglieri L & Scarpa S (2015) Are pharmacogenomic biomarkers an effective tool to predict taxane toxicity and outcome in breast cancer patients? Literature review. *Cancer Chemother Pharmacol* **76**, 679–690.
36 Hayes CL, Spink DC, Spink BC, Cao JQ, Walker NJ & Sutter TR (1996) 17 beta-estradiol hydroxylation catalyzed by human cytochrome P450 1B1. *Proc Natl Acad Sci USA* **93**, 9776–9781.
37 Liehr JG (1990) Genotoxic effects of estrogens. *Mutat Res* **238**, 269–276.
38 Go RE, Hwang KA & Choi KC (2015) Cytochrome P450 1 family and cancers. *J Steroid Biochem Mol Biol* **147**, 24–30.
39 Kamel M, Shouman S, El-Merzebany M, Kilic G, Veenstra T, Saeed M, Wagih M, Diaz-Arrastia C, Patel D & Salama S (2012) Effect of tumour necrosis factor-alpha on estrogen metabolic pathways in breast cancer cells. *J Cancer* **3**, 310–321.
40 Bandapalli OR, Ehrmann F, Ehemann V, Gaida M, Macher-Goeppinger S, Wente M, Schirmacher P & Brand K (2012) Down-regulation of CXCL1 inhibits tumor growth in colorectal liver metastasis. *Cytokine* **57**, 46–53.
41 Wang Y, Qu Y, Niu XL, Sun WJ, Zhang XL & Li LZ (2011) Autocrine production of interleukin-8 confers cisplatin and paclitaxel resistance in ovarian cancer cells. *Cytokine* **56**, 365–375.
42 Chen Q, Zhang XH & Massague J (2011) Macrophage binding to receptor VCAM-1 transmits survival signals in breast cancer cells that invade the lungs. *Cancer Cell* **20**, 538–549.
43 Wang B, Guo P & Auguste DT (2015) Mapping the CXCR4 receptor on breast cancer cells. *Biomaterials* **57**, 161–168.
44 Marsigliante S, Vetrugno C & Muscella A (2013) CCL20 induces migration and proliferation on breast epithelial cells. *J Cell Physiol* **228**, 1873–1883.
45 Marsigliante S, Vetrugno C & Muscella A (2016) Paracrine CCL20 loop induces epithelial-mesenchymal transition in breast epithelial cells. *Mol Carcinog* **55**, 1175–1186.
46 Lerebours F, Vacher S, Andrieu C, Espie M, Marty M, Lidereau R & Bieche I (2008) NF-kappa B genes have a major role in inflammatory breast cancer. *BMC Cancer* **8**, 41.
47 Gehrmann M, Schmidt M, Brase JC, Roos P & Hengstler JG (2008) Prediction of paclitaxel resistance in breast cancer: is CYP1B1*3 a new factor of influence? *Pharmacogenomics* **9**, 969–974.
48 McKay JA, Melvin WT, Ah-See AK, Ewen SW, Greenlee WF, Marcus CB, Burke MD & Murray GI (1995) Expression of cytochrome P450 CYP1B1 in breast cancer. *FEBS Lett* **374**, 270–272.
49 Saini S, Hirata H, Majid S & Dahiya R (2009) Functional significance of cytochrome P450 1B1 in endometrial carcinogenesis. *Cancer Res* **69**, 7038–7045.

Supporting information

Additional Supporting Information may be found online in the supporting information tab for this article:

Fig. S1. Clustering analysis for gene transcription which were influenced by low-dose PTX.
Table S1. Primer sequences for real-time PCR.

Graphical Abstract

The contents of this page will be used as part of the graphical abstract of html only. It will not be published as part of main.

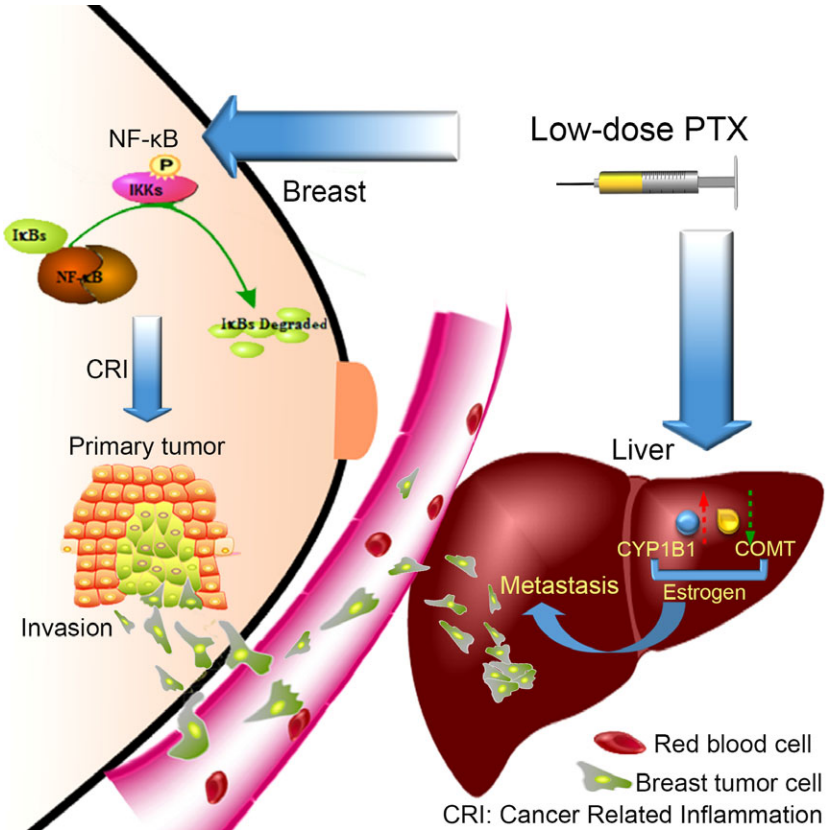

We report that low doses of paclitaxel have tumour-supportive and pro-metastatic effects in breast cancer cells and the host hepatic microenvironment. Treating breast cancer cells with a low dose of paclitaxel promoted NF-κB-dependent inflammation and metastasis. Furthermore, low doses of paclitaxel induced changes in host hepatic estrogen metabolism. As a result, we observed increased liver metastasis of breast cancer cells in mouse xenograft models.